

PHYSICOCHEMICAL PROBLEMS  
OF MATERIALS PROTECTION

# Electrochemical Assessment of Inhibitive Behavior of Some Antibacterial Drugs on 316 Stainless Steel in Acidic Medium<sup>1</sup>

H. M. El-Abbasy<sup>a</sup>, Ahmed Abdel Nazeer<sup>b, \*</sup>, and A. S. Fouda<sup>a</sup>

<sup>a</sup>Department of Chemistry, Faculty of Science, El-Mansoura University, El-Mansoura-5516, Egypt

<sup>b</sup>National Research Centre, Electrochemistry Laboratory, Dokki, Cairo 12622, Egypt

\*e-mail: anazeer\_nrc@yahoo.com

Received May 2, 2015

**Abstract**—In this work, the inhibitive effect of some antibacterial drugs against the corrosion of 316 stainless steel in 1M HCl has been studied by weight loss, potentiodynamic polarization and electrochemical impedance spectroscopy (EIS). The inhibiting effect explained by adsorption of the additives on steel surface. The inhibition efficiency increases with increasing the inhibitors concentrations and decreases with increasing the temperature. The data obtained fit well to Langmuir adsorption isotherm and the kinetic-thermodynamic model. The results of polarization studies indicate that the investigated antibacterial drugs are mixed type inhibitors. Increasing the inhibition efficiency of the investigated inhibitors with the addition of iodide ions indicates that iodide ions play important role in the adsorption process. The efficiencies obtained from the different electrochemical techniques were in good agreement which prove the validity of these tools in the measurements of the tested inhibitors.

DOI: 10.1134/S2070205116030084

## 1. INTRODUCTION

Because iron and its alloys are the backbone of industrial constructions, many research projects have been concerned with their stability. One of most important task is the retardation of their attack by acid solutions used during pickling, industrial cleaning and descaling. The use of additive is one of the major solutions for this problem. Hence, various additives are used to protect iron and its alloy against corrosive attack. The most effective and efficient inhibitors are the organic compounds that have  $\pi$  bonds, heteroatoms (P, S, N, and O), and inorganic compounds such as chromate, dichromate, nitrite, and so on [1–6]. However, the major problem associated with most of these inhibitors is that they are not ecofriendly as they contain heavy metals and other toxic compounds [7]. Green corrosion inhibitors are biodegradable and do not contain toxic substances [8–10]. Thus, the development of the novel corrosion inhibitors of natural source and non-toxic type has been considered to be more important and desirable [11]. Because of their natural origin [12–14], as well as their non-toxic characteristics [15] and due to its negligible effect on the environment [16]. Drugs seem to be ideal candidates to replace traditional toxic corrosion inhibitors. Several drugs such as: Cefazidime, Cefepime, Cefoperazone [17, 18], Ciprofloxacin, Norfloxacin [19], Rhodanine azosulpha [20] have been studied for the

corrosion inhibition of 304 stainless steel in acidic media. Synergism is an effective method to improve the inhibitive performance. The synergistic inhibition effects of organic inhibitor/metallic ion mixture [21–30] on corrosion of steel in acidic media have also been studied. Hydrochloric acid was chosen as it is extensively used in industries, the most important fields of application being acid pickling, industrial acid cleaning, acid descaling and oil well acidizing [31].

This study aims to gain some insight into the corrosion of 316 stainless steel in HCl in the presence and absence of some antibacterial drugs as inhibitors using chemical and electrochemical techniques. Additionally, thermodynamic data were obtained from adsorption isotherms and Arrhenius plots. These drugs were chosen as corrosion inhibitors due to: (a) higher molecular size (b)  $\pi$ -electron contribution of the benzene rings and (c) presence of more active adsorption sites.

## 2. EXPERIMENTAL

### 2.1. Materials and Reagents

The aggressive solutions, 1 M HCl were prepared from an analytical grade 37% HCl, by dilution with bi-distilled water. All the experiments were performed with 316 stainless steel samples of the following composition (wt %): 0.08% C, 2% Mn, 0.04% P, 0.03% S, 0.75% Si, 16–18% Cr, 11–14% Ni, 2–3% Mo and balance iron. Stock solutions ( $10^{-3}$  M) of inhibitors,

<sup>1</sup> The article is published in the original.

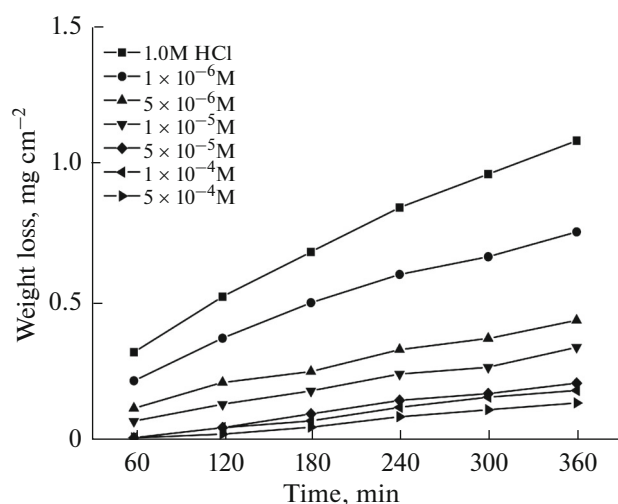


**Fig. 1.** Plots of weight loss vs. time for the corrosion of 316 stainless steel in 1 M HCl without and with different concentrations of compound (3) at 25°C.

1 M KI and 1 M NaCl were prepared by dissolving appropriate weights in bi-distilled water. The investigated antibacterial drugs were obtained from different Egyptian companies and of analytical-reagent (AR) grade. Schem. 1 shows their chemical molecular structures.

### 2.2. Weight Loss Method

The 316 stainless steel sheets of  $2 \times 2 \times 0.2$  cm were abraded with a series of emery paper up to 1200 grit and washed with bi-distilled water then with acetone and dried between filter paper. After weighing accurately, the specimens were immersed in 250 mL beaker containing 100 mL HCl without and with addition of different concentrations of the studied inhibitors. All the aggressive acid solutions were open to air. After the specific period of time, the specimens were taken out washed dried, and weighed accurately. In order to get good reproducibility experiments were carried out in triplicate. The average weight loss of three parallel stainless steel 316 sheets was obtained. The inhibition efficiency (I%) and the degrees of surface coverage ( $\theta$ ) of the investigated compounds were calculated from the following equation:

$$I\% = \theta \times 100 = [(W_0 - W)/W_0] \times 100, \quad (1)$$

where  $W_0$  and  $W$  are the values of the average weight loss without and with addition of the inhibitor, respectively. Scheme.

### 2.3. Potentiodynamic Polarization Method

Electrochemical polarization experiments were carried out in a conventional three-electrode cell with a capacity of 100 mL. A platinum counter electrode and a saturated calomel electrode (SCE) coupled to a

fine Luggin capillary as the reference electrode. To minimize the ohmic contribution the Luggin capillary was kept close to the working electrode. The working electrode was in the form of a square stainless steel embedded in PVC holder using epoxy resin so that the flat surface was the only surface in the electrode. The working electrode area was  $1 \times 1$  cm, was abraded with emery paper up to 1200 grit, rinsed with bi-distilled water, degreased with acetone, and dried with a cold air stream. A time interval of about 30 minutes was given for the system to attain a steady state and the open circuit potential (OCP) was noted. All experiments were carried out at  $25 \pm 1^\circ\text{C}$  using circulating thermostat and solutions were not deaerated. For polarization measurements potential from  $-300$  to  $100$  mV (relative to open circuit potential,  $E_{OC}$ ) was applied while potential from  $-500$  to  $700$  mV (relative to reference electrode potential,  $E_{ref}$ ) was applied in case of pitting measurements. I% and the degree of surface coverage ( $\theta$ ) were defined as:

$$I\% = \theta \times 100 = [(i_{corr} - i_{corr(inh)})/i_{corr}] \times 100 \quad (2)$$

where  $i_{corr}$  and  $i_{corr(inh)}$  are the uninhibited and inhibited corrosion current density values, respectively, determined by extrapolation of Tafel lines to the corrosion potential.

### 2.4. Electrochemical Impedance Spectroscopy (EIS) Method

EIS experiments were conducted at  $25 \pm 1^\circ\text{C}$  at the OCP after immersion the electrode for 30 minutes in the test solution. The AC signal was 5 mV peak to peak and the frequency range studied was between 100 kHz and 0.2 Hz.

The inhibition efficiency (I%) and the surface coverage ( $\theta$ ) of the investigated inhibitors obtained from the impedance measurements can be calculated by applying the following relation:

$$I\% = \theta \times 100 = [1 - (R_{ct}^0/R_{ct})] \times 100, \quad (3)$$

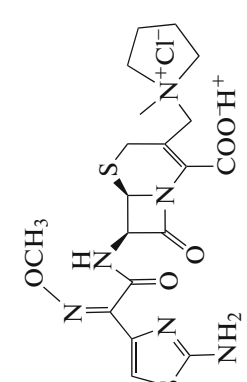
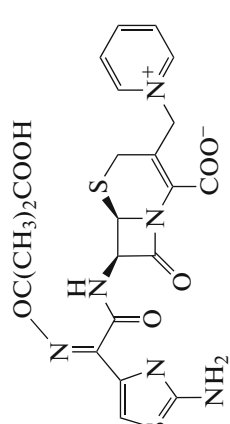
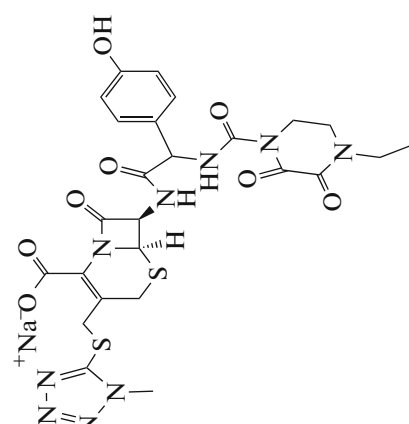
where  $R_{ct}^0$  and  $R_{ct}$  are the charge transfer resistance in the absence and presence of inhibitor, respectively. Electrochemical experiments were carried out using Potentiostat/Galvanostat/Zra analyzer (Gamry PCI300/4). A personal computer with DC 105 software for polarization, EIS300 software for impedance and Echem Analyst v. 5.21 was used for data fitting and calculating.

## 3. RESULTS AND DISCUSSIONS

### 3.1. Weight—Loss Measurements

Figure 1 shows the effect of increasing concentrations of inhibitor (3) on the weight loss-time curves of type 316 stainless steel at  $25^\circ\text{C}$ . Similar curves (not shown) were obtained for the other two inhibitors. It is

**Scheme 1.** Shows structures, names, chemical formula and molecular weights of the investigated antibacterial drugs

Comp.	Structures	Names	Produced by	Chemical formula	Mol. wt
1		(6R,7R,Z)-7-(2-(2-aminothiazol-4-yl)-2-(methoxyimino)acetamido)-3-(1-methyl pyrrolidinium-1-yl)methyl)-8-oxo-5-thia-1-aza-bicyclo[4.2.0]oct-2-ene-2-carboxylate	Bristol-Myers Squibb Egypt Company, Egypt	$C_{19}H_{25}ClN_6O_5S_2$	517.02
2		(6R,7R,Z)-7-(2-(2-aminothiazol-4-yl)-2-(2-carboxypropan-2-ylxyimino)acetamido)-8-oxo-3-(pyridinium-1-ylmethyl)-5-thia-1-aza-bicyclo[4.2.0]oct-2-ene-2-carboxylate	Glaxo Smithkline Company, Egypt	$C_{22}H_{22}N_6O_7S_2$	546.58
3		(6R,7R,Z)-7-([2-[(4-ethyl-2,3-dioxo-piperazine-1-carbonyl)amino]-2-(4-hydroxyphenyl)acetyl]amino]-3-[(1-methyltetrazol-5-yl)sulfanyl]methyl)-8-oxo-5-thia-1-aza-bicyclo[4.2.0]oct-2-ene-2-carboxylic acid	Pharco Pharmaceutical Company, Egypt	$C_{25}H_{26}N_9NaO_8S_2$	667.65

**Table 1.** Number of active sites ( $1/y$ ), slopes of Langmuir isotherm lines, equilibrium constant of the adsorption reaction ( $K$ ) and free energy of adsorption ( $\Delta G_{\text{ads}}^{\circ}$ ) of inhibitors and heat of adsorption ( $Q$ ) of  $5 \times 10^{-5}$  M of compounds 1, 2 and 3 on 316 stainless steel surface in 1 M HCl at 25°C

Comp.	Kinetic model			Langmuir isotherm			$-Q$ (kJ mol <sup>-1</sup> )
	$1/y$	$K \times 10^5$	$-\Delta G_{\text{ads}}^{\circ}$ (kJ mol <sup>-1</sup> )	slope	$K \times 10^5$	$-\Delta G_{\text{ads}}^{\circ}$ (kJ mol <sup>-1</sup> )	
1	2.2	1.0	38.4	1.2	1.5	39.5	10.6
2	2.4	3.1	41.3	1.2	2.5	40.8	14.0
3	2.1	3.5	41.6	1.1	2.7	41.0	20.9

obvious that the weight loss of type 316 stainless steel in the presence of inhibitors varies linearly with time, and is much lower than that obtained in blank solution. The linearity obtained indicated the absence of insoluble surface film during corrosion and that the inhibitors were first adsorbed onto the metal surface and, therefore, impede the corrosion process [32].

The values of I % and corrosion rate (CR) obtained from weight loss method at different concentrations of inhibitors at 25°C are summarized in Table 1. The I% determined from weight loss was found to decrease in the following order: (3) > (2) > (1).

### 3.1.1. Adsorption Isotherm

The adsorption on the corroding surfaces never reaches the real equilibrium and tends to reach an adsorption steady state. When corrosion rate is sufficiently decreased in the presence of inhibitor, the adsorption steady state has a tendency to attain quasi-equilibrium adsorption in thermodynamic was using

the appropriate adsorption isotherm. Various adsorption isotherms were tested to find the best suitable adsorption isotherm for adsorption of the studied inhibitors on the surface of 316 stainless steel in 1 M HCl solution. Various adsorption isotherms were applied to fit  $\theta$  values (obtained by using Eq. (2)) but the best fit was found to obey Langmuir adsorption isotherm [33] which may be expressed by:

$$C/\theta = 1/\beta + C, \quad (4)$$

where  $C$  is inhibitor concentration and  $\beta$  is equilibrium constant of adsorption. It is well known that the standard adsorption free energy ( $\Delta G_{\text{ads}}^{\circ}$ ) is related to equilibrium constant of adsorption ( $\beta$ ) and ( $\Delta G_{\text{ads}}^{\circ}$ ) can be calculated by the following equation [34]:

$$\beta = 1/55.5 \exp[-\Delta G_{\text{ads}}^{\circ}/RT]. \quad (5)$$

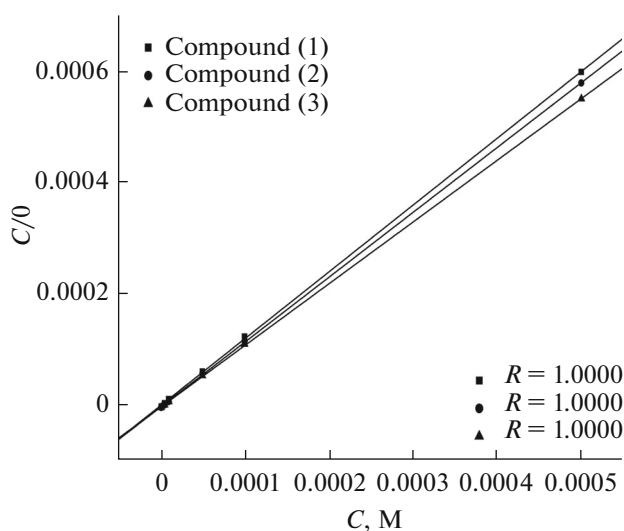


**Fig. 2.** Langmuir adsorption isotherm plotted as  $(C/\theta)$  vs. Conc. of compounds (1), (2) and (3) for the corrosion of 316 stainless steel in 1 M HCl at 25°C.

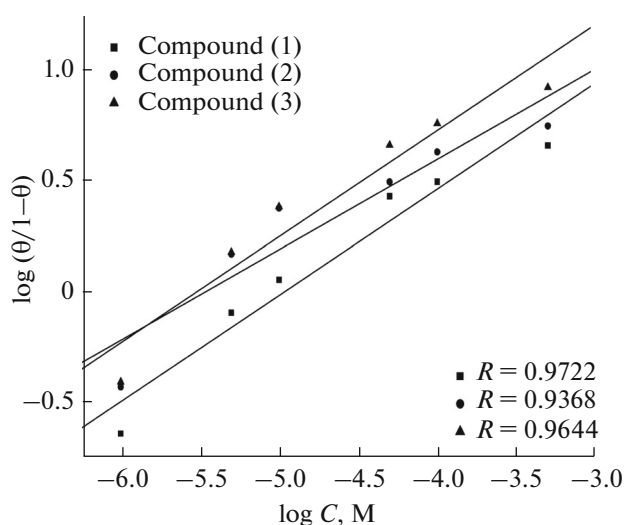


**Fig. 3.** El-Awady model plotted as  $\log(\theta/(1-\theta))$  vs.  $\log C$  of compounds (1), (2) and (3) for the corrosion of 316 stainless steel in 1 M HCl at 25°C.

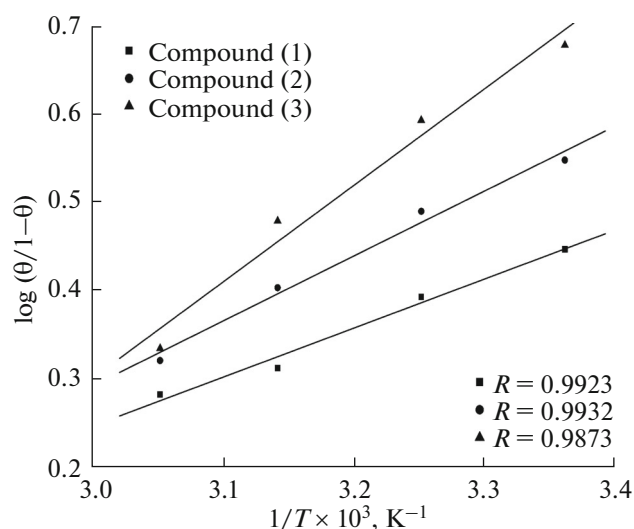


**Fig. 4.** Plots of  $\log(\theta/1-\theta)$  vs.  $1/T$  for  $5 \times 10^{-5}$  M of compounds (1), (2) and (3) for the corrosion of 316 stainless steel in 1 M HCl at 25°C.

Figure 2 represents the plot of  $(C/\theta)$  against  $C$  for all studied compounds. Also, it is found that the kinetic-thermodynamic model of El-Awady et al [35].

$$\log(\theta/1-\theta) = \log k' + y \log C, \quad (6)$$

is valid to operate the present adsorption data.  $\beta = \beta'(1/y)$ ,  $\beta'$  is constant and  $1/y$  is the number of the surface active sites occupied by one inhibitor molecule and  $C$  is the bulk concentration of the inhibitor. Plotting  $\log(\theta/1-\theta)$  against  $\log C$  for the studied compounds is given in Fig. 3. Straight-line relationships were obtained suggesting the validity of this model for the studied case. A plot of  $\log(\theta/1-\theta)$  vs.  $1/T$  at constant additives concentration ( $5 \times 10^{-5}$  M) (Fig. 4) gives straight lines according to the following equation:

$$\log \theta/1-\theta = \log A + \log C - (Q/2.303RT). \quad (7)$$

The  $Q$  values were obtained from the slopes of these lines. The values of  $K$  and  $\Delta G_{\text{ads}}^{\circ}$  calculated by Langmuir isotherm and  $1/y$ ,  $\beta$  and  $\Delta G_{\text{ads}}^{\circ}$  calculated by the kinetic model and the values of  $Q$  are given in Table 1. The negative values of  $\Delta G_{\text{ads}}^{\circ}$  suggest that the adsorption of inhibitors molecules onto steel surface is a spontaneous process. The magnitude of adsorption heat reaches the magnitude of chemical reaction heat, which is the result of the transference of electron from donating atoms in the inhibitor molecule to the  $d$ -orbital of the iron atom. The negative values of  $Q$  show that the process of adsorption is exothermal. It is noting that the value of  $1/y$  is more than unity. This means that the given inhibitor molecules will form monolayer on the steel surface. In general the values of  $\Delta G_{\text{ads}}^{\circ}$  obtained from El-Awady et al model are com-

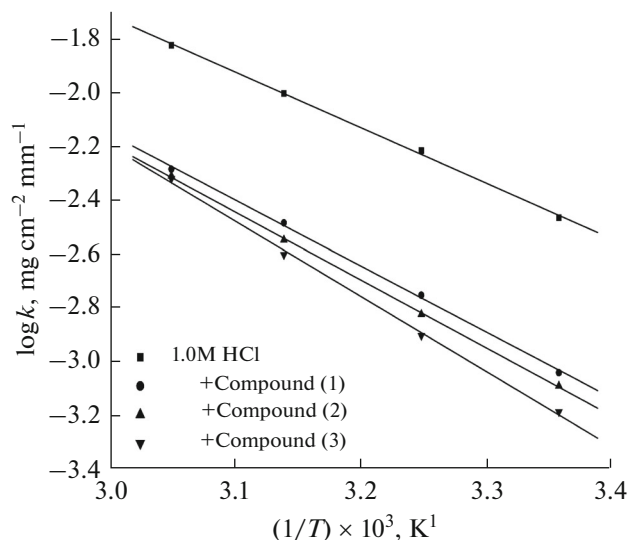


**Fig. 5.** Arrhenius plots ( $\log k$  vs.  $1/T$ ) for 316 stainless steel in 1 M HCl in the absence and presence of  $5 \times 10^{-5}$  M of compounds (1), (2) and (3).

parable with those obtained from Langmuir isotherms.

### 3.1.2. Effect of Temperature

In order to study the effect of temperature on the inhibition characteristic of all the studied compounds, weight loss measurements were performed at different temperatures from 25 to 25°C in the absence and presence of different concentrations of the investigated inhibitors for 6 h immersion time. The calculated values of the percentage inhibition efficiency ( $I\%$ ) are listed in Table 2. Inspection of Table 2 reveals that, the inhibition efficiency increases with an increase in inhibitor concentration and decrease with raising the temperature. This behavior could be attributed to the increase of the number of adsorbed molecules at the metal surface. At one and the same inhibitors concentration the % IE decreases in the following order: (3) > (2) > (1).

The adsorption process was well elucidating by using a thermodynamic model, in addition a kinetic thermodynamic model was another tool to explain the mechanism of corrosion inhibition for an inhibitor.

The apparent effective activation energies ( $E_a^*$ ) for the corrosion reaction of 316 stainless steel in 1 M HCl solution and presence of different concentrations of the studied compounds were calculated from Arrhenius type equation [36]:

$$\log k_{\text{corr}} = \log A - E_a^*/(2.303 RT), \quad (8)$$

where  $A$  is the Arrhenius pre-exponential factor. A plot of  $\log k_{\text{corr}}$  versus  $1/T$  at  $5 \times 10^{-5}$  M from the studied

**Table 2.** Effect of temperature on the inhibition efficiencies of different concentrations of compounds 1, 2 and 3 for corrosion of 316 stainless steel in 1 M HCl

Temp., °C	Conc., M	I%		
		Compound (1)	Compound (2)	Compound (3)
25	$1 \times 10^{-6}$	19.0	27.6	28.6
	$5 \times 10^{-6}$	45.2	60.2	60.8
	$1 \times 10^{-5}$	53.7	71.0	71.3
	$5 \times 10^{-5}$	73.5	76.3	82.5
	$1 \times 10^{-4}$	76.3	81.5	85.5
	$5 \times 10^{-4}$	82.4	85.2	89.6
35	$5 \times 10^{-6}$	39.2	55.3	55.9
	$1 \times 10^{-5}$	44.7	66.4	66.9
	$5 \times 10^{-5}$	71.0	75.4	79.5
	$1 \times 10^{-4}$	75.8	78.3	84.5
	$5 \times 10^{-4}$	82.7	85.1	91.1
45	$5 \times 10^{-6}$	33.1	38.7	47.1
	$1 \times 10^{-5}$	40.3	57.3	60.4
	$5 \times 10^{-5}$	67.0	71.5	74.9
	$1 \times 10^{-4}$	71.4	76.5	81.1
	$5 \times 10^{-4}$	81.4	82.7	89.1
55	$5 \times 10^{-6}$	25.9	31.3	27.6
	$1 \times 10^{-5}$	33.9	45.0	45.1
	$5 \times 10^{-5}$	65.5	67.5	68.2
	$1 \times 10^{-4}$	67.3	70.0	75.0
	$5 \times 10^{-4}$	77.4	78.1	85.6

compounds was shown in Fig. (5), straight lines were obtained. The values of  $E_a^*$  can be obtained from the slope of the straight lines. Free energies of activation ( $\Delta G^*$ ) were calculated by applying the Eyring equation [37]:

$$K = (K'T/h)e^{-\Delta G^*/RT}. \quad (9)$$

Another convenient form of equation 9 is equation 10:

$$\Delta G^* = RT \left[ \ln \frac{K'T}{h} - \ln k \right], \quad (10)$$

where,  $k$  is the corrosion rate,  $h$  is Planck's constant,  $K'$  is Boltzmann's constant,  $R$  is the universal gas constant and  $T$  is the absolute temperature. The enthalpy of activation ( $\Delta H^*$ ) and the entropy of activation ( $\Delta S^*$ ) were calculated by applying the following equations [38]:

$$\Delta H^* = E_a^* - RT, \quad (11)$$

$$\Delta S^* = \frac{\Delta H^* - \Delta G^*}{T}. \quad (12)$$

The calculated values of activation energy and thermodynamic activation parameters ( $\Delta G^*$ ,  $\Delta H^*$ ,  $\Delta S^*$ ) for the dissolution of 316 stainless steels in 1 M HCl are listed in Table 3. It is obvious that the activation energy is higher in the presence of the additives than in their absence. Similar results were obtained by other authors [39–41]. The higher values of  $E_a^*$  in the presence of the studied compounds indicates that physical adsorption or weak chemical bonding between the inhibitor molecules and the steel surface may occur [42].  $E_a^*$  being more than  $-40 \text{ kJ mol}^{-1}$  and less than  $-80 \text{ kJ mol}^{-1}$ , is between the threshold values for physical adsorption and chemical adsorption indicates that the adsorption of the inhibitors on the steels surfaces involves two types of interaction. The activation energy of blank solution is comparable with other reported values [43]. The values of  $\Delta G^*$  and  $\Delta H^*$  are

positive and high in the presence of the inhibitors over that of the uninhibited solution. This implies that energy barrier of the corrosion reaction in the presence of the investigated inhibitors increases. On the other hand,  $\Delta S^*$  values are lower and negative in presence of the inhibitors, this means that addition of these compounds cause a decrease in the disordering in going from reactants to the activated complexes [44, 45]. It is evident that the values of  $(\Delta G^*)$  increase with increasing temperature where the constantly values of  $(\Delta H^*)$  indicated that the mechanism of the corrosion reaction was not changed by raising the temperatures from 25 to 55°C. The order of decreasing activation energy and thermodynamic activation parameters in the presence of the investigated inhibitors agrees with the order of decreasing I% of these compounds.

### 3.2. Potentiodynamic Polarization Measurements

Anodic and cathodic polarizations were carried out potentiodynamic for stainless steel 316 in 1 M HCl solution in the absence and presence of various concentrations of the studied compounds at 25°C. The results are represented in Fig. 6 for compound (3), similar behaviors were obtained for other compounds (not shown). The obtained potentiodynamic polarization parameters are given in Table 4. These results indicate that the cathodic and anodic curves obtained exhibit Tafel-type behavior. Additionally, the form of these curves is very similar either in the cathodic or in the anodic side, which indicates that the mechanisms of stainless steel dissolution and hydrogen reduction apparently remain unaltered in the presence of these additives. Addition of the studied compounds decreased both the cathodic and anodic current densities and caused mainly parallel displacement to the more negative and positive values, respectively, i.e. the presence of the studied compounds solution inhibits both the hydrogen evolution and the anodic dissolution processes with overall shift of  $E_{\text{corr}}$  to more negative values with respect to the OCP.

The results also show that the slopes of the anodic and the cathodic Tafel slopes ( $\beta_a$  and  $\beta_c$ ) were slightly changed on increasing the concentration of the tested compounds. This indicates that there is no change of the mechanism of inhibition in presence and absence of inhibitors. The values of  $\beta_c$  are slightly higher than the values of  $\beta_a$  suggesting a cathodic action of the inhibitor. This could be interpreted as an action of mixed inhibitor control over the electrochemical semi-reactions. This means that the investigated compounds are mixed type inhibitors, but the cathode is more preferentially polarized than the anode. The higher values of Tafel slope can be attributed to surface kinetic process rather the diffusion-controlled process [46]. The constancy and the parallel of cathodic slope obtained from the electrochemical measurements indicate that the hydrogen evolution reaction was activation controlled [47] and the addition of these deriv-

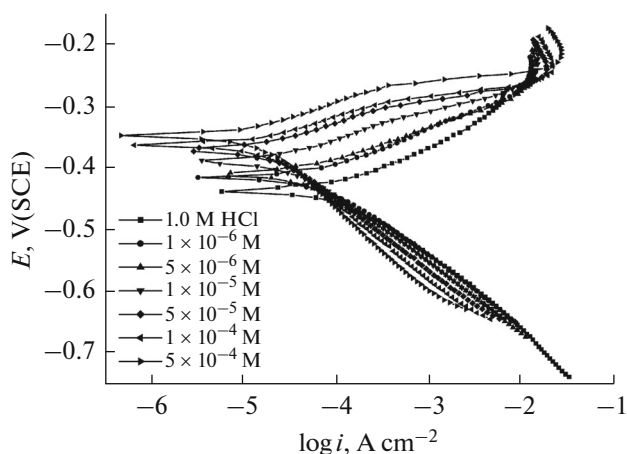


**Fig. 6.** Potentiodynamic polarization curves of 316 stainless steel in 1 M HCl in the absence and presence of different concentrations of compound 3 at 25°C.

atives did not modify the mechanism of this process. This result suggests that the inhibition mode of the studied compounds was by simple blockage of the sur-

**Table 3.** Activation energy and thermodynamic activation parameters for dissolution of 316 stainless steel in 1 M HCl in the absence and presence of  $5 \times 10^{-5}$  M of compounds 1, 2 and 3 at different temperatures

Comp.	Thermodynamic activation parameters	Temperature, °C			
		25	35	45	55
1.0 M HCl	$E_a^*$ (kJ mol <sup>-1</sup> )	39.47			
	$\Delta G^*$ (kJ mol <sup>-1</sup> )	86.97	88.50	90.16	91.95
	$\Delta H^*$ (kJ mol <sup>-1</sup> )	36.99	36.91	36.83	36.74
	$-\Delta S^*$ (J mol <sup>-1</sup> K <sup>-1</sup> )	167.7	167.5	167.7	168.3
1	$E_a^*$ (kJ mol <sup>-1</sup> )	46.82			
	$\Delta G^*$ (kJ mol <sup>-1</sup> )	90.26	91.67	93.10	94.85
	$\Delta H^*$ (kJ mol <sup>-1</sup> )	44.34	44.26	44.18	44.09
	$-\Delta S^*$ (J mol <sup>-1</sup> K <sup>-1</sup> )	154.1	153.9	153.8	154.8
2	$E_a^*$ (kJ mol <sup>-1</sup> )	48.18			
	$\Delta G^*$ (kJ mol <sup>-1</sup> )	90.70	92.09	93.48	95.02
	$\Delta H^*$ (kJ mol <sup>-1</sup> )	45.70	45.62	45.54	45.45
	$-\Delta S^*$ (J mol <sup>-1</sup> K <sup>-1</sup> )	151.0	150.9	150.8	151.1
3	$E_a^*$ (kJ mol <sup>-1</sup> )	53.38			
	$\Delta G^*$ (kJ mol <sup>-1</sup> )	91.29	92.56	93.82	95.07
	$\Delta H^*$ (kJ mol <sup>-1</sup> )	50.90	50.82	50.74	50.65
	$-\Delta S^*$ (J mol <sup>-1</sup> K <sup>-1</sup> )	135.5	135.5	135.5	135.4

**Table 4.** Effect of concentration of compounds 1, 2 and 3 on the electrochemical parameters, surface coverage ( $\theta$ ) and inhibition efficiency (I%) of 316 stainless steel in 1 M HCl at 25°C

Comp.	Conc., M	$-E_{\text{corr}}$ , mV vs. SCE	$i_{\text{corr}}$ , $\mu\text{A cm}^{-2}$	$-\beta_c$ , mV dec $^{-1}$	$\beta_a$ , mV dec $^{-1}$	$R_p$ , ohm cm $^2$	CR, mm y $^{-1}$	$\theta$	I%
1	1.0 M HCl	437	116.2	119	79	177.2	1.349	—	—
	$1 \times 10^{-6}$	438	129.3	119	80	160.5	1.501	0.113	11.3
	$5 \times 10^{-6}$	424	80.1	114	66	227.3	0.929	0.311	31.1
	$1 \times 10^{-5}$	417	73.6	115	61	235.0	0.854	0.367	36.7
	$5 \times 10^{-5}$	391	22.7	101	49	635.9	0.263	0.805	80.5
	$1 \times 10^{-4}$	376	16.9	104	45	807.7	0.196	0.855	85.5
	$5 \times 10^{-4}$	374	16.1	103	43	824.6	0.186	0.861	86.1
2	$1 \times 10^{-6}$	423	71.3	111	67	253.9	0.827	0.386	38.6
	$5 \times 10^{-6}$	413	64.5	112	64	273.2	0.748	0.445	44.5
	$1 \times 10^{-5}$	405	26.4	97	50.2	544.6	0.306	0.773	77.3
	$5 \times 10^{-5}$	386	16.4	97	46	823.1	0.190	0.859	85.9
	$1 \times 10^{-4}$	381	15.0	100	44	888.2	0.174	0.871	87.1
	$5 \times 10^{-4}$	370	14.4	103	44	930.1	0.167	0.876	87.6
3	$1 \times 10^{-6}$	416	65.6	110	68	278.6	0.761	0.435	43.5
	$5 \times 10^{-6}$	410	44.1	109	55	360.3	0.512	0.620	62.0
	$1 \times 10^{-5}$	389	24.6	104	51	598.4	0.286	0.788	78.8
	$5 \times 10^{-5}$	370	15.5	109	47	915.5	0.180	0.867	86.7
	$1 \times 10^{-4}$	363	13.3	115	49	1118.0	0.154	0.886	88.6
	$5 \times 10^{-4}$	349	11.9	131.0	55.4	1424.0	0.138	0.898	89.8

**Table 5.** Effect of addition of  $1 \times 10^{-2}$  M of KI on the inhibition efficiencies of different concentrations of compounds 1, 2 and 3 for the corrosion of 316 stainless steel in 1 M HCl at 25°C

Comp. Conc., M	I% from $i_{\text{corr}}$					
	compound (1)		compound (2)		compound (3)	
	without KI	with KI	without KI	with KI	without KI	with KI
$1 \times 10^{-6}$	—11.3	88.1	38.6	88.9	43.5	89.5
$5 \times 10^{-6}$	31.1	89.3	44.5	90.1	62.0	91.1
$1 \times 10^{-5}$	36.7	89.6	77.3	91.0	78.8	92.3
$5 \times 10^{-5}$	80.5	91.4	85.9	91.4	86.7	92.7
$1 \times 10^{-4}$	85.5	92.1	87.1	91.2	88.6	93.2
$5 \times 10^{-4}$	86.1	93.3	87.6	90.8	89.8	93.0



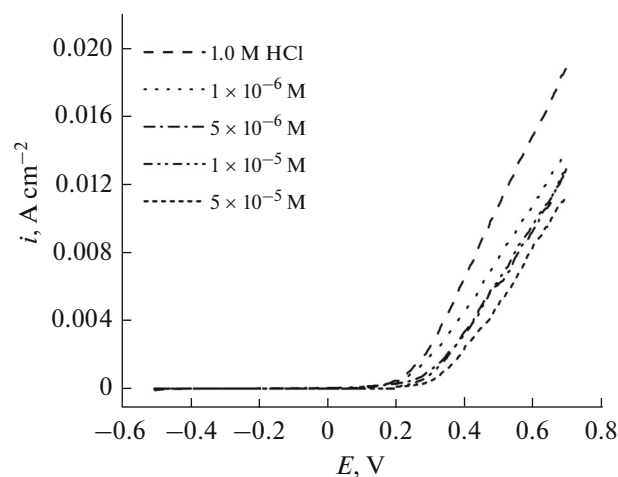


**Fig. 7.** Potentiodynamic anodic curves for 316 stainless steel in 0.1 M NaCl in the absence and presence of different concentrations of compound 3 at 25°C.

face by adsorption. The order of decreased inhibition efficiency for the additives is: (3) > (2) > (1).

### 3.3. Synergistic Effect

The effect of addition  $1 \times 10^{-2}$  M KI on the corrosion rate of stainless steel 316 in absence and presence of different concentrations of the studied compounds in 1 M HCl solution was investigated using potentiodynamic polarization method. Results of I% of the studied compounds without and with KI are summarized in Table 5. It was observed from these results that the presence of  $I^-$  improved the I% of the studied compounds significantly. The interactions of KI with the studied compounds can be described by introduction of the synergistic parameter ( $S_\theta$ ) which is defined as [48]:

$$S_\theta = 1 - \theta_{1+2} / (1 - \theta'_{1+2}), \quad (13)$$

**Table 6.** Synergism parameter ( $S_\theta$ ) for different concentrations of compounds 1, 2 and 3 with  $1 \times 10^{-2}$  M KI for the corrosion of 316 stainless steels in 1 M HCl at 25°C

Inhibitor Conc., M + $1 \times 10^{-2}$ M KI	Synergism parameter ( $S_\theta$ ), $i_{\text{corr}}$		
	compound (1)	compound (2)	compound (3)
$1 \times 10^{-6}$	1.366	0.806	0.784
$5 \times 10^{-6}$	0.940	0.818	0.622
$1 \times 10^{-5}$	0.889	0.368	0.402
$5 \times 10^{-5}$	0.331	0.239	0.268
$1 \times 10^{-4}$	0.268	0.214	0.245
$5 \times 10^{-4}$	0.301	0.197	0.213

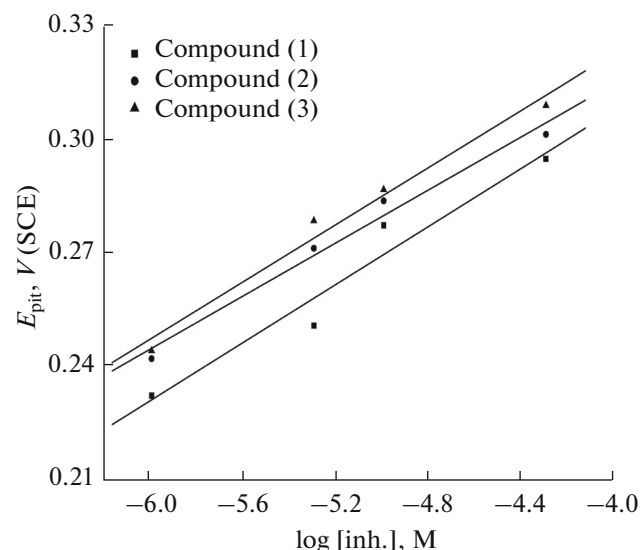


**Fig. 8.** Pitting potential;  $E_{\text{pit}}$  as a function of concentration of compounds (1), (2) and (3) for the corrosion of 316 stainless steel in 0.1 M NaCl at 25°C.

where  $\theta_{1+2} = (\theta_1 + \theta_2) - (\theta_1\theta_2)$ ,  $\theta_1$  = surface coverage by anion,  $\theta_2$  = surface coverage by cation and  $\theta'_{1+2}$  = measured surface coverage by both the anion and cation.  $S_\theta$  approaches 1 when no interaction between the inhibitor compounds exists, while  $S_\theta > 1$  points to a synergistic effect. In the case of  $S_\theta < 1$ , the antagonistic interaction prevails. Values of  $S_\theta$  summarized in Table 6 are less than unity, suggesting that the phenomenon of antagonistic interaction exists between  $I^-$  and the studied compounds. Similar results obtained elsewhere [29].

The order of increasing inhibition efficiency for the studied compounds in the presence of  $1 \times 10^{-2}$  M KI with different concentration of the inhibitors for stainless steel 316 in 1 M HCl is as follows: 3 > 2 > 1.

**Table 7.** Electrochemical kinetic parameters obtained by EIS technique for the corrosion of 316 stainless steel in 1 M HCl at different concentrations of inhibitors 1, 2 and 3 at 25°C

Comp.	Conc., M	$C_{dl}$ , $\mu\text{F cm}^{-2}$	Phase degree	$R_{ct}$ ohm $\text{cm}^2$	$\theta$	I%
1	1.0 M HCl	85.5	69.3	281.5	—	—
	$5 \times 10^{-6}$	78.3	69.9	282.4	0.003	00.3
	$1 \times 10^{-5}$	62.0	73.4	508.2	0.446	44.6
	$5 \times 10^{-5}$	50.7	74.4	618.0	0.544	54.4
	$5 \times 10^{-4}$	37.6	76.7	973.4	0.711	71.1
2	$5 \times 10^{-6}$	72.7	71.6	404.6	0.304	30.4
	$1 \times 10^{-5}$	66.1	71.6	471.6	0.403	40.3
	$5 \times 10^{-5}$	52.8	74.7	949.3	0.703	70.3
	$5 \times 10^{-4}$	44.2	74.8	1188.0	0.763	76.3
3	$5 \times 10^{-6}$	85.9	71.7	355.2	0.207	20.7
	$1 \times 10^{-5}$	54.3	72.7	552.3	0.490	49.0
	$5 \times 10^{-5}$	35.4	76.3	1125.0	0.750	75.0
	$5 \times 10^{-4}$	30.3	77.7	1538.0	0.817	81.7

### 3.4. Potentiodynamic Anodic Measurements (Pitting Corrosion)

The passive film formed spontaneously on austenitic stainless steels has been widely studied using surface analysis techniques [49–51]. A mixture of iron and chromium oxides is formed, with hydroxide and  $\text{H}_2\text{O}$ -containing compounds concentrated in the outermost region of the film and chromium oxide enrichment in the inner region (metal/film interface). Thus the passive film formed on the stainless steel surface consists of an inner Cr(III)-oxide/hydroxide layer and a very thin outer layer of Fe(II)/(III)-oxide/hydroxide [52].

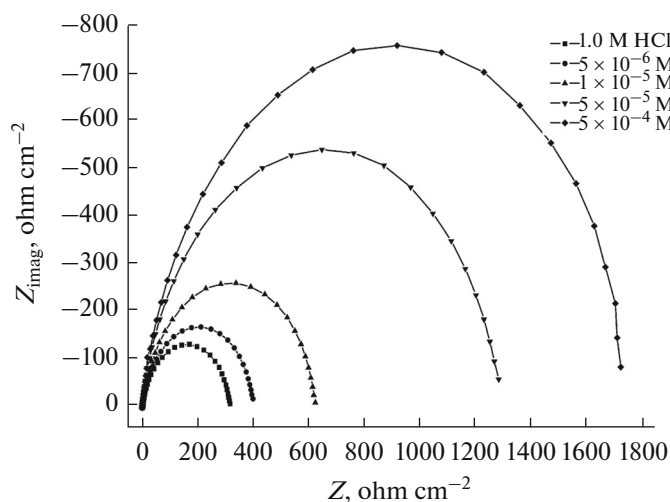


**Fig. 9.** The Nyquist plots for the corrosion of 316 stainless steel in 1 M HCl in the absence and presence of different concentrations of compound 3 at 25°C.

The effect of adding different concentrations of the studied compounds on the pitting corrosion behavior of stainless steel 316 in 0.1 NaCl solution was investigated by potentiodynamic polarization measurements. The addition of the inhibitors increases the breakdown potential towards more positive potential (Fig. 7), i.e. inhibits pitting corrosion of the steel.

Figure 8 shows the relation between  $E_{pit}$  and the inhibitors concentrations, straight lines obtained according to the following equation:

$$E_{pit} = a' + b' \log[\text{inh.}] \quad (14)$$

Symbols  $a'$  and  $b'$  are constants. The increase of the inhibitors concentration increases the pitting potential to more positive values, i.e. decreases the pitting corrosion. The adsorption of the inhibitors on the steels surfaces can prevent the adsorption of  $\text{Cl}^-$  ion (which is responsible for pitting corrosion). Pitting potentials; the order of decreasing  $E_{pit}$  of stainless steel 316 in the presence of the studied compounds is agree with the order of decreasing I% of these compounds, obtained from weight loss and potentiodynamic measurements.

### 3.5. Electrochemical Impedance Spectroscopy (EIS)

EIS measurements were carried out for corrosion behavior of stainless steel 316 in 1 M HCl solution in the absence and presence of various concentrations of the studied compounds at  $25 \pm 1^\circ\text{C}$ . The obtained Nyquist plot for compound (3) is shown in Fig. 9 similar curves were obtained for inhibitor (1, 2) (not shown). The impedance diagrams have an approximately semicircular appearance shows that the corrosion of stainless steel 316 is controlled by a charge transfer process. The diameters of the capacitive loop

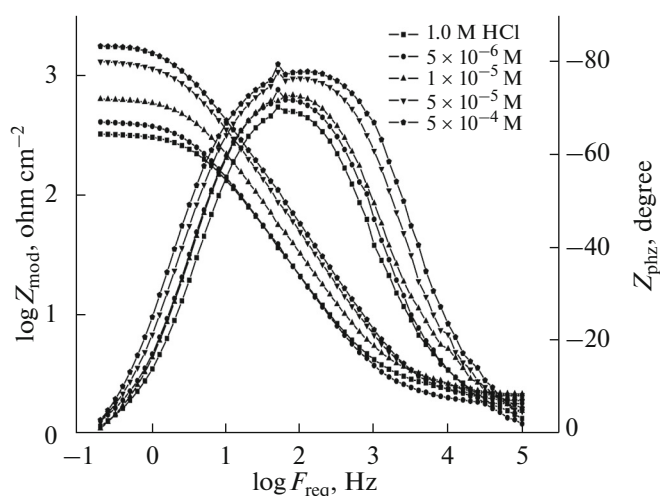


**Fig. 10.** The Bode plots for the corrosion of 316 stainless steel in 1 M HCl in the absence and presence of different concentrations of compound 3 at 25°C.

obtained increases in the presence of the inhibitors and were indicative of the degree of inhibition of the corrosion process. The Bode plot of compound (3) is shown in Fig. 10 the high frequency limits corresponds to the solution resistance  $R_s$  ( $\Omega$ ), while the lower frequency limits corresponds to  $(R_{ct} + R_s)$ . The low frequency contribution shows the kinetic response of the charge transfer reaction [53]. The impedance parameter such as charge transfer resistance ( $R_{ct}$ ), double layer capacitance ( $C_{dl}$ ) and inhibition efficiency (I%) were calculated and are listed in Table 7. The result obtained show that the value of charge transfer resistance ( $R_{ct}$ ) for stainless steel 316 in HCl solution changed after the addition of inhibitors. The  $R_{ct}$  values increases and the  $C_{dl}$  values decreases with increasing the concentrations of the studied compounds. This leads to an increase of percent inhibition (I%). The high  $R_{ct}$  values associated with slower corroding system [54]. The inhibition efficiency obtained from impedance measurements are in good agreement with those obtained from weight loss and potentiodynamic polarization studies (3) > (2) > (1).

### 3.6. Mechanism of Inhibition

The investigated inhibitors confer high protection to stainless steel 316 corrosion in 1 M HCl and function through adsorption on the metal surface following Langmuir isotherm. The obtained results by weight loss, potentiodynamic polarization and electrochemical impedance spectroscopy (EIS) techniques indicate that the extent of corrosion inhibition of the investigated compounds followed the following order: (3) > (2) > (1). It can be explained on the basis of adsorption. It is apparent from the molecular structure that, these compounds can be adsorbed on the metal surface

through the lone pair of electrons of oxygen and/or nitrogen and/or sulfur atoms and delocalized  $\pi$ -electrons of benzene ring. The difference in the inhibition efficiencies can be explained on the basis of the type and the number of hetero atoms in the cavity of these compounds. Also the inhibition efficiency values can be explained on the basis of the molecular weight; compound (3) exhibits excellent inhibition efficiency due to its molecular weight (667.65) that may facilitate better surface coverage. Compound (2) comes after compound (3) in inhibition efficiency because it has lesser molecular weight (546.58). Compound (1) has the lowest inhibition efficiency; this is because it has the lowest molecular weight (517.02) and has no aromatic ring.

## CONCLUSIONS

From the results of the study we can concluded that the investigated compounds are efficient inhibitors for 316 stainless steel in 1 M HCl. The adsorption of these compounds on the steel surface was found to obey Langmuir adsorption isotherm. Polarization data shows that the studied antibacterial drugs act as mixed-type inhibitors in 1 M HCl. The presence of KI improves the inhibition efficiency, indicating presence of a synergistic effect between these studied compounds and the iodide anion. Thermodynamic adsorption parameters show that the studied inhibitors are adsorbed on the alloy surface by an endothermic, spontaneous process. The values of inhibition efficiencies obtained from the different independent quantitative techniques used are in good agreement and showed the validity of the studied techniques.

## REFERENCES

1. Lece, H.D., Emregul, K.C., and Atakol, O., *Corros. Sci.*, 2008, vol. 50, p. 1460.
2. Mu, G., Li, X., Qu, Q., and Zhou, J., *Corros. Sci.*, 2006, vol. 48, p. 445.
3. Samiento-Bustos, E., Gonzalez Rodriguez, J.G., Uru-churtu, J., et al., *Corros. Sci.*, 2008, vol. 50, p. 2296.
4. Bastos, A.C., Ferreira, M.G., and Simoes, A.M., *Corros. Sci.*, 2006, vol. 48, p. 1500.
5. Sahin, M., Gece, G., Karci, F., et al., *J. Appl. Electrochem.*, 2008, vol. 38, p. 809.
6. Fouda, A.S., Abdel Nazeer, A. Ibrahim, M., et al., *J. Korean Chem. Soc.*, 2013, vol. 57, p. 272.
7. Eddy, N.O. and Ebenso, E.E., *Afr. J. Pure Appl. Chem.*, 2008, vol. 2, p. 1.
8. Abdel Nazeer, A., El-Abbasy, H.M., and Fouda, A.S., *Res. Chem. Intermed.*, 2013, vol. 39, p. 921.
9. Okafor, P.C., Osabor, V.I., and Ebenso, E.E., *Pigm. Resin Technol.*, 2007, vol. 36, p. 299.
10. Umoren, S.A. and Ebenso, E.E., *Pigm. Resin Technol.*, 2008, vol. 37, p. 173.
11. Raja, P.B. and Sethuraman, M.G., *Mater. Lett.*, 2008, vol. 62, p. 113.

12. Newman, D.J., Cragg, G.M., and Snader, K.M., *J. Nat. Prod.*, 2003, vol. 66, p. 1022.
13. Newman, D.J. and Cragg, G.M., *J. Nat. Prod.*, 2007, vol. 70, p. 461.
14. Harvey, A.L., *Drug Discov. Today*, 2008, vol. 13, p. 894.
15. Struck, S., Schmidt, U., Gruening, B., et al., *Genome Inform.*, 2008, vol. 20, p. 231.
16. Enick, O.V., *MSc Thesis*, Burnaby: Simon Fraser Univ., 2006.
17. Abdel Nazeer, A., El-Abbasy, H.M., and Fouda, A.S., *J. Mater. Eng. Perf.*, 2013, vol. 22, p. 2314.
18. Fouda, A.S., Mostafa, H.A., and El-Abbasy, H.M., *J. Appl. Electrochem.*, 2010, vol. 40, p. 163.
19. Dubey, R.S. and Potdar, Y., *Indian J. Chem. Tech.*, 2009, vol. 16, p. 334.
20. Abdallah, M., *Corros. Sci.*, 2002, vol. 44, p. 717.
21. Singh, D.D.N., Singh, T.B., and Gaur, B., *Corros. Sci.*, 1995, vol. 37, p. 1005.
22. Mu, G.N., Zhao, T.P., Liu, M., et al., *Corrosion*, 1996, vol. 52, p. 853.
23. Wahdan, M.H., *Mater. Chem. Phys.*, 1997, vol. 49, p. 135.
24. Wahdan, M.H. and Gomma, G.K., *Mater. Chem. Phys.*, 1997, vol. 47, p. 176.
25. Abdallah, M. and El-Naggar, M.M., *Mater. Chem. Phys.*, 2001, vol. 71, p. 291.
26. Cheng, S., Chen, S.G., Liu, T., et al., *Electrochim. Acta*, 2007, vol. 52, p. 5932.
27. Li, X.H., Deng, S.D., Mu, G.N., and Qu, Q., *Mater. Lett.*, 2007, vol. 61, p. 2514.
28. Li, X.H., Deng, S.D., Fu, H., et al., *Appl. Surf. Sci.*, 2008, vol. 254, p. 5574.
29. Li, X.H., Deng, S.D., Fu, H., et al., *Corros. Sci.*, 2008, vol. 50, p. 2635.
30. Li, X.H., Deng, S.D., Fu, H., et al., *Corros. Sci.*, 2008, vol. 50, p. 3599.
31. Abdel Nazeer, A., Shalabi, K., and Fouda, A.S., *Res. Chem. Intermed.*, 2015, vol. 41, p. 4833.
32. Abdallah, M., *Corros. Sci.*, 2004, vol. 46, p. 1981.
33. Langmuir, I., *J. Am. Chem. Soc.*, 1917, vol. 39, p. 1848.
34. Khamis, E., *Corrosion*, 1990, vol. 46, p. 476.
35. El-Awady, Y.A. and Ahmed, A.I., *Indian J. Chem., Sect. A: Inorg., Bioinorg., Phys., Theor. Anal. Chem.*, 1985, vol. 24, p. 601.
36. Putilova, I.N., Balezin, S.A., and Barannik, V.P., *Metallic Corrosion Inhibitors*, New York: Pergamon, 1960, p. 31.
37. Stevens, P. and Phil, M., *Chemical Kinetics*, London: Chapman and Hall, 1970.
38. Banerjee, S.N., *An Introduction to Science of Corrosion and Its Inhibition*, New Delhi: Oxanion, 1985.
39. Zhao, T.P. and Mu, G.N., *Corros. Sci.*, 1999, vol. 41, p. 1937.
40. Fouda, A.S., Mostafa, H.A., El-Taib, F., et al., *Corros. Sci.*, 2005, vol. 47, p. 1988.
41. Fouda, A.S., Al-Sawary, A.A., Ahmed, F.Sh., et al., *Corros. Sci.*, 2009, vol. 51, p. 485.
42. Popova, A., Sokolova, E., Raicheva, S., et al., *Corros. Sci.*, 2003, vol. 45, p. 33.
43. Sanad, S.H., Esmail, A., and Mahmoud, M.A., *J. Mater. Sci.*, 1992, vol. 27, p. 5706.
44. Riggs, O.L. and Hurd, R.M., *Corrosion*, 1967, vol. 23, p. 252.
45. Gomma, G.K. and Wahdan, M.H., *Mater. Chem. Phys.*, 1995, vol. 39, p. 209.
46. Mohamed, A.K., Mostafa, H.A., El-Awady, G.Y., et al., *Port. Electrochim. Acta*, 2000, vol. 18, p. 99.
47. El-Ouafi, A., Hammouti, B., Oudda, H., et al., *Anti-Corrosion Meth. Mater.*, 2002, vol. 49, p. 199.
48. Aramaki, K., Hagiwera, M., and Nishihara, H., *Corros. Sci.*, 1987, vol. 27, p. 487.
49. Polo, J.L., Cano, E., and Bastidas, J.M., *J. Electroanal. Chem.*, 2002, vol. 537, p. 183.
50. Abreu, C.M., Cristobal, M.J., Novoa, X.R., et al., *Electrochim. Acta*, 2004, vol. 49, p. 3049.
51. El-Egamy, S.S. and Badaway, W.A., *J. Appl. Electrochem.*, 2004, vol. 34, p. 1153.
52. Cosman, N.P., Fatih, K., and Roscoe, S.G., *J. Electroanal. Chem.*, 2005, vol. 574, p. 261.
53. Mansfeld, F., *Electrochim Acta*, 1990, vol. 35, p. 1533.
54. Babic-Samardzija, K., Lupu, C., and Hackerman, N., *Langmuir*, 2005, vol. 21, p. 12187.